2002

Evaporating Heat Transfer Of R22 And R410A In 9.52 mm Smooth And Microfin Tubes

M. H. Kim
Samsung Electronics Company

J. S. Shin
Pohang University of Science and Technology

B. H. Lim
Samsung Electronics Company

R8-4

Evaporating Heat Transfer of R22 and R410A in 9.52mm Smooth and Microfin Tubes

Man-Hoe Kim[1], Jeong-Seob Shin[2], Byung-Han Lim[3]

[1,3]R&D Center, Samsung Electronics Company, 416 Maetan-3Dong, Suwon, 442-742, Korea.

[2]Department of Mechanical Engineering, POSTECH, San 31 Hyoja-Dong, Pohang, Kyungbuk 790-784, Korea.

ABSTRACT

An experimental investigation of evaporating heat transfer in 9.52 mm horizontal copper tubes was conducted. The refrigerants tested were R22 and the near-azeotropic mixture, R410A. The test rig had a straight, horizontal test section with an active length of 0.92 m and was heated by the heat transfer fluid (hot water) circulated in a surrounding annulus. Constant heat flux of 11.0 kW/m^2 was maintained and refrigerant quality varied from 0.2 to 0.8. The results were reported for evaporation at 15°C in a 0.92 m long test section for 30-60 kg/h mass flow rate. The local and average heat transfer coefficients for seven microfin tubes were presented compared to those for a smooth tube. The average evaporation heat transfer coefficients of R22 and R410A for the microfin tubes were 86-227 percent and 64-199 percent, respectively, higher than those for the smooth tube. When compared to R22 at the same test conditions, the evaporating heat transfer coefficients for R410A were 97-129 percent of R22.

NOMENCLATURE

A	: Heat transfer area, mm^2
c_p	: Specific heat, J/kg-K
D_i	: Inner diameter, mm
D_{ai}	: Average inner diameter, mm
h	: Heat transfer coefficient, W/m^2-K
H_f	: Fin height, mm
i	: Enthalpy, J/kg
i_f	: Saturation liquid enthalpy, J/kg
i_{fg}	: Latent heat of evaporation, J/kg
k	: Thermal conductivity, W/m-K
m_r	: Refrigerant mass flow rate, kg/s
m_w	: Water mass flow rate, kg/s
MF	: Microfin tube
ΔP	: Pressure drop, Pa
Q	: Heat transfer rate, W
q_i''	: Heat flux, W/m^2
R_w	: Conductive thermal resistance, K/W
ST	: Smooth tube
T	: Temperature, K
ΔT	: Temperature difference, K
r	: Refrigerant side
s	: Saturation
t	: Bottom wall thickness, mm
x	: Refrigerant vapor quality
U	: Overall heat transfer coefficient, W/m^2-K
W_t	: Mean wall thickness, mm

Greek letters

α	: Apex angle, deg.
β	: Helix angle, deg.
η	: Efficiency index defined
η_h	: Heat transfer enhancement factor

Subscripts

av	: Average
i	: Iinner side
in	: Inlet
o	: Outside
out	: Outlet
p	: Plane tube
ph	: Preheater
s	: Saturation
ts	: Test section
w	: Tube wall

INTRODUCTION

Heat exchangers in air conditioning and heat pump applications play an important role on system efficiency and physical size, and on environmental impacts. Finned round tube heat exchangers are usually used for the evaporator and condenser for residential air-conditioning systems. The air-side thermal resistance of the heat exchangers dominates the total thermal resistance. To improve the thermal performance of finned tube heat exchangers, it is necessary to reduce air-side thermal resistance. To investigate the overall performance of the finned tube heat exchangers, however, tube-side heat transfer and pressure drop behaviors as well as air-side performance must be considered simultaneously. Several investigators [1-14] performed studies on evaporation in microfin round tubes.

Hitachi [1,2] appears to be the first to develop microfin tubes for heat exchnagers for air-conditioning and heat pump systems. Yasuda et al. [3] developed "THERMOFIN-HEX TUBE", which was 9.52 mm o.d. microfin tube with 18° degree helix angle, to improve the evaporation performance of room air conditioners. They reported R22 evaporation heat transfer coefficient had a maximum at mass flux of 200-250 kg/m^{2}s. Schlager et al. [4] investigated evaporation and condensation heat transfer and pressure drop characteristics in three horizontal 12.7 mm microfin tubes with R22. They found evaporation and condensation heat transfer coefficients in the microfin tubes were 1.6-2.2 and 1.5-2.0 times, respectively, larger than those in the smooth tubes. Kandlikar [5] presented a flow boiling heat transfer correlation for enhanced tubes by modifying his smooth tube correlation, and Chritoffersen et al. [6] investigated local evaporation heat transfer and pressure drop characteristics for R22, R134a and R32/R125 (60/40%) in smooth and microfin tubes. Kaul et al. [7] conducted a study on the horizontal evaporation heat transfer performance of R22 and several alternative refrigerants in a fluid heated microfin tube and they developed correlations of heat transfer coefficients for each refrigerant. Chamra et al. [8] presented R22 evaporation heat transfer and pressure drop data for new microfin geometries applied to the inner surface of 15.88 mm o.d. tubes. Kuo et al. [9] reported the effect of heat flux, mass flux and evaporation pressure on the heat transfer coefficients using 9.52 mm o.d. microfin and plain tubes. Liu [10] performed a study of evaporation and condensation heat transfer and pressure drop behaviors of R134a and R22 in a 9.52 mm o.d. axially grooved tube and presented heat transfer coefficient and pressure drop correlations for each refrigerant. Uchida et al. [11] performed an experimental study on the R407C evaporation in a smooth, single- and cross-grooved tubes. They repoted that heat transfer coefficients for the cross-grooved tube are over three times and 20-40% larger than those for the smooth and single-grooved tubes, respectively. Yamamoto et al. [12] carried out the R410A evapoation test in horizontal tubes and proposed the correlation of evaporation heat transfer coefficients for R410A. Kattan et al. [13] developed a heat transfer model which includes the effects of two-phase flow pattern. The model is based on experimental data taking into account the physical mechanism occuring during evaporation. Boissieux et al. [14] performed an experimental study on evaporation of HFC refrigerants in a horizontal smooth tube. They found that the Kattan et al.'s model [13] predicted well the local heat transfer data during the whole evaporating process. They developed a heat transfer model based on Kattan et al.'s model and the modifed model offered a good prediction of the test data, with a standard deviation of 6.1%. However, there was little experimental data available for various tube geometries for R410A refrigerant.

This study investigates local and average two-phase heat transfer characteristics during R22 and R410A evaporation in a smooth and seven different microfin tubes. The test results are compared to those for a round tube at the same mass flow rate.

EXPERIMENTS

Test apparatus

Fig. 1 shows schematic diagram of the test apparatus. It consists of circulation loops for the refrigerant and heat transfer fluids and data acquisition system. The refrigerant circulation loop includes a gear pump, a mass flow meter, a pre-heater, a test section, a stabilizer, a sub-cooling unit and a receiver. The refrigerant is delivered to the test section by the magnetic gear pump. The refrigerant flow rate was measured using a coriolis mass flow meter with a nominal flow range of 0 ~135 kg/h and an accuracy of ±0.15%. The refrigerant quality at the inlet of the test section is regulated through heat exchange between the refrigerant and the hot water in the pre-heater.

The test section consists of two concentric, circular tubes. The refrigerant is flowing through the inner copper tube, and the heat-transfer fluid (water) is flowing in the counter direction to the refrigerant through the annular space. Table 1 describes the simple cross-sectional configuration and geometrical parameters for the test tubes. The outer diameter of the copper tubes tested is 9.52 mm and the test section has an effective length of 920 mm. The outer tube is acrylic circular tube with the inner diameter of 18.0 mm. Thermocouples and pressure transducers are inserted in the inlet and outlet of the test tube and a differential pressure sensor is connected between them. The measured saturation temperatures were in good agreement with the temperature calculated based on the measured saturated pressure within ±0.3°C. To measure the tube wall temperatures, twelve thermocouples were attached on the outer surface of the tube at three locations along the length of the tube, mounted at the top, bottom, right and left of the tube in the circumferential direction. The entire refrigeration circulation loop including the test section was wrapped with 40 mm thick foam insulation to minimize heat transfer between refrigerant and the environment. The energy balance between the inside and outside of the test tube was checked using water at the proper heat flux, and the results showed agreement within 3%.

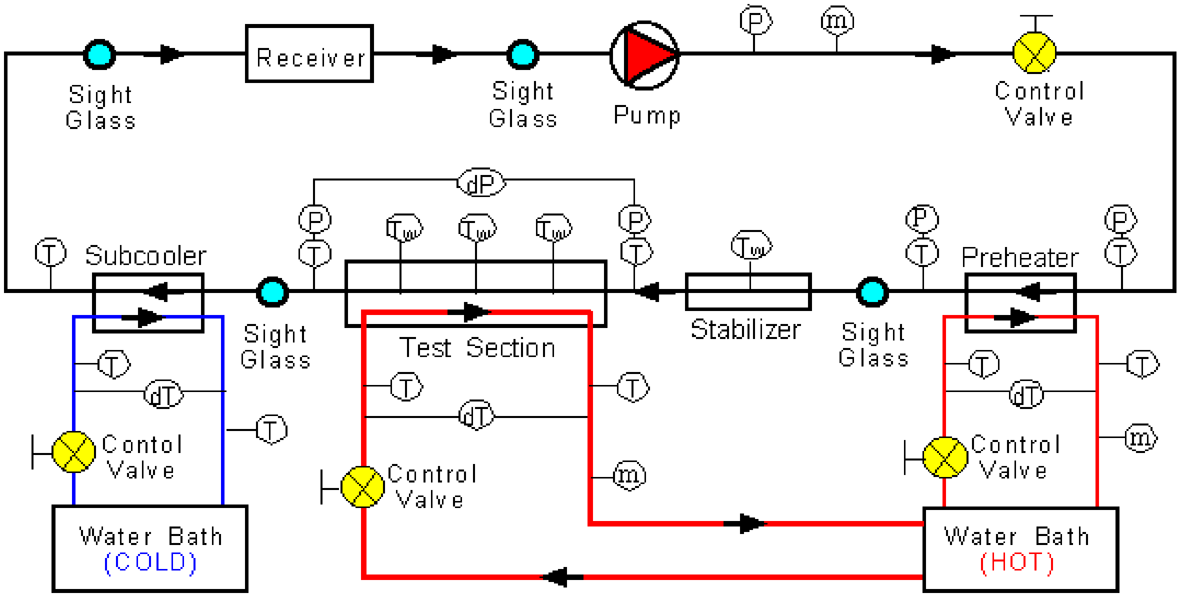

Fig. 1 Schematic of the experimental apparatus.

Table 1 Specifications of the test tubes (Outer diameter: 9.52 mm).

Tube Types		Fin geometries	D_i (mm)	D_{ai} (mm)	t (mm)	W_t (mm)	H_f (mm)	β (°)	α (°)	Number of fins	H_f/D_i	A/A_p
Smooth tube	ST	-	8.70	8.70	0.41	0.41	-	-	-	-	-	1.0
Single-groove	MF-1		8.68	8.82	0.30	0.35	0.12	25	-	60	0.0138	1.28
	MF-2		8.52	8.80	0.30	0.36	0.20	18	53	60	0.0235	1.51
	MF-3		8.52	8.80	0.30	0.36	0.20	18	40	60	0.0235	1.60
	MF-4		8.47	8.80	0.28	0.36	0.25	15.5	25	65	0.0295	1.85
	MF-5		8.46	8.80	0.30	0.36	0.23 0.16	30	40	54	0.0272 0.0189	1.53
Cross-groove	MF-6		8.14	8.60	0.37	0.46	0.32	25	-	20	0.0393	-
	MF-7		8.51	8.80	0.30	0.36	0.20	44	15	72	0.0235	-

The hot and cold water circulation loops to control the state of the refrigerant include a pre-heater and a sub-cooler. Thermocouples were inserted to measure the temperatures at the inlet and outlet of the sub-cooler and pre-heater, and thermopiles were attached to measure the temperature differences between the inlet and outlet of the hot and cold water. Heat transfer rate of the pre-heater was regulated by water flow rate measured using a coriolis mass flow meter with a nominal flow range of 0 ~ 1225 kg/h and an accuracy ±0.15%.

The test data were collected using a hybrid recorder and analyzed in real time with a PC running the data reduction program. All the information about test conditions and test data during the test, were displayed on the monitor and test conditions were changed based on this information.

Test condition and method

The test conditions described in Table 2 span the range of operating conditions of an evaporator for a residential air conditioning system. The tests are conducted for evaporation at 15°C for 30, 45 and 60 kg/h mass flow rate with R22 and R410A. The refrigerant flow rate is controlled by regulating the input power of the variable speed magnetic gear pump. Constant heat flux of 11 kW/m^2 based on the average inside tube surface area is maintained through all the tests. The quality of the refrigerant entering the test section is controlled through the heat exchange rate in the pre-heater, and the heat flux was maintained by regulating the water flow rate from the hot water bath. The test conditions and data to be collected were monitored throughout the test, and data sets of 60-100 were recorded and averaged over 6-10 minutes after test conditions reached the steady state.

Table 2 Test conditions.

Refrigerants	R22, R410A
Evaporating temp. (^{o}C)	15
Heat flux (kW/m^2)	11.0
Mass flow rate (kg/h)	30, 45, 60
Quality range	0.2-0.8

Table 3 Estimated uncertainties.

Items	Accuracy
Temperature	±0.1 ^{o}C
Pressure	±0.2 %
Mass flow	±0.15 %
Refrigerant quality	±3.2 ~ ±6.3 %
Average heat transfer coefficient	±6.5 ~ ±12.3 %

Data reduction

Evaporating heat transfer coefficient (h) can be obtained from the following equation

$$\frac{1}{U_o A_o} = \frac{1}{h_o A_o} + R_w + \frac{1}{hA} = LMTD / Q \tag{1}$$

where Q is the heat transfer rate at the test section

$$Q = m_w c_p \Delta T \tag{2}$$

$$LMTD = \frac{\Delta T_1 - \Delta T_2}{\ln(\Delta T_1 / \Delta T_2)} \tag{3}$$

$$\Delta T_1 = T_{s,in} - T_{o,out} \ , \ \Delta T_2 = T_{s,out} - T_{o,in} \tag{4}$$

The Modified Wilson Plot method [15, 16] is used to get the heat transfer coefficients of annular side for the test section. Wilson plot data are obtained for the water flow rate of annular side of 110-200 kg/h as shown in Fig. 2.

Heat transfer coefficient can be obtained also from the measured wall temperatures.

$$h = \frac{q_i''}{T_w - T_r} \tag{5}$$

Where q_i'' is heat flux, T_w and T_r are inside wall and refrigerant temperatures, respectively. Heat flux was determined using inside tube wall area, based on the average of root and minimum inner diameters and heat transfer rate (Q) obtained from Eq. (2). T_w was calculated from the temperature measured at the outside tube wall using the one-dimensional conduction equation, approximated as Cartesian geometry.

The average and inlet qualities of the refrigerant at the test section were calculated from the energy balance in the preheater and the test section, respectively

$$x = x_i + \frac{Q_{ts}}{2m_r i_{fg}} \tag{6}$$

$$x_i = \frac{1}{i_{fg}}\left(\frac{Q_{ph}}{m_r} - (i_f - i_{ph,i})\right) \tag{7}$$

Average heat transfer coefficients were obtained from the average values of the integral of the local heat transfer coefficient, which were fitted over the quality ranges of 0.2-0.8. Refrigerant properties were calculated using REFPROP [17]. Accounting for all instrument errors, uncertainties for the average heat transfer coefficients were estimated 12.3% (see Table 3) using the standard method [18].

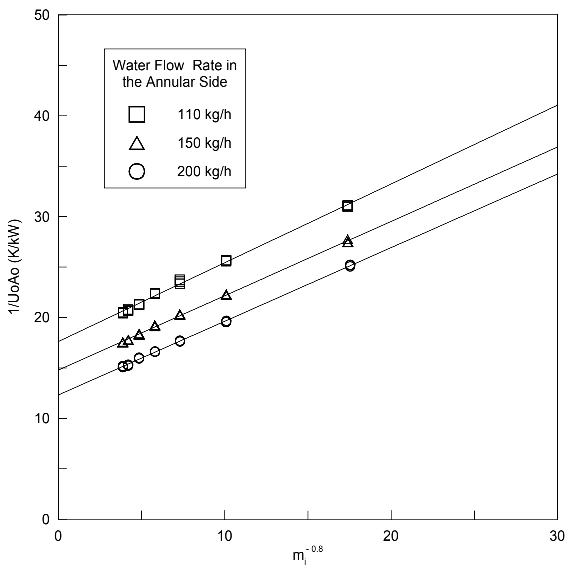

Fig. 2 Wilson plot data for the annular side.

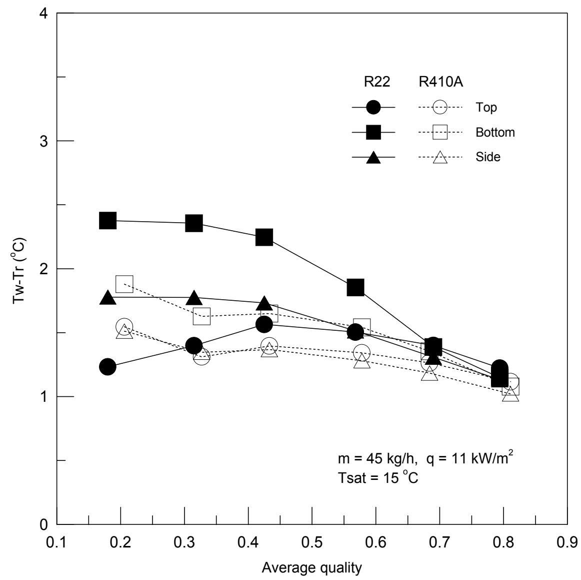

Fig. 4 Wall temperaure profiles for MF-2.

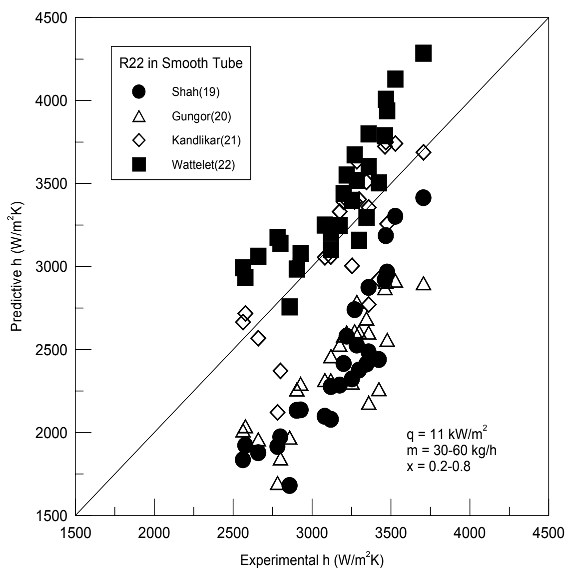

Fig. 3 Heat transfer coefficients for the plane tube.

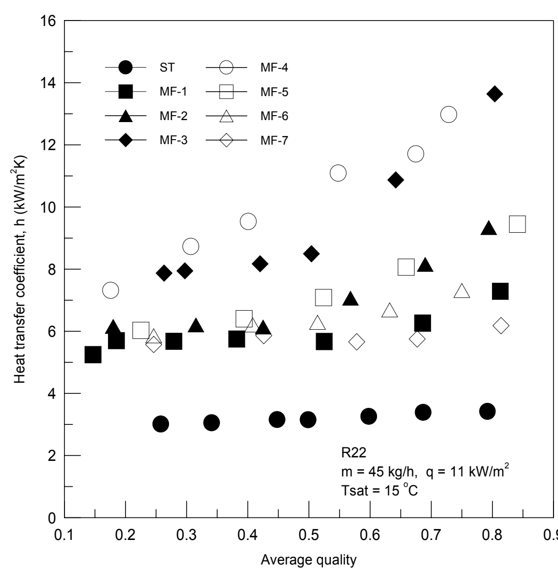

Fig. 5 Local heat transfer coefficients for R22.

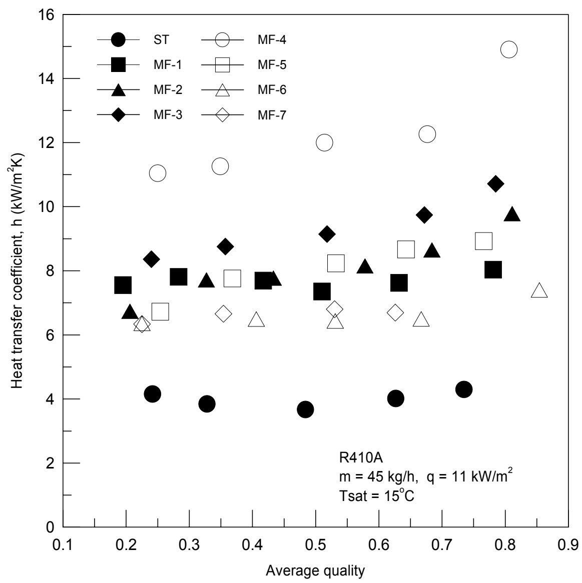

Fig. 6 Local heat transfer coefficients for R410A.

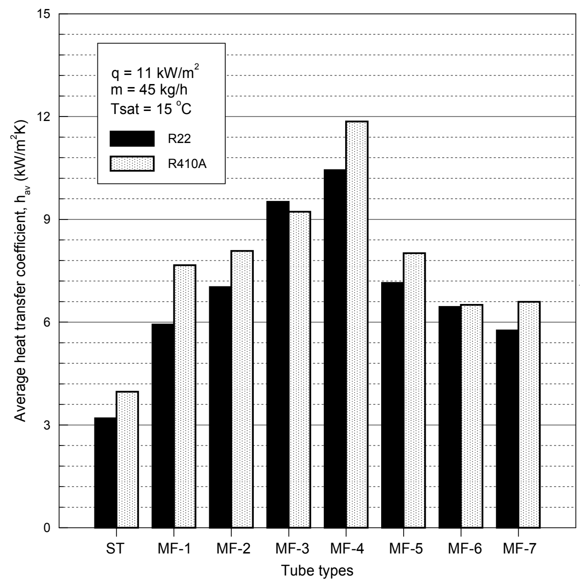

Fig. 7 Average evaporation heat transfer coefficients.

Table 4 Heat transfer enhancement factor (η_h) at the mass flow rate of 45 kg/h.

	ST	MF-1	MF-2	MF-3	MF-4	MF-5	MF-6	MF-7
R22	1.0	1.86	2.20	2.98	3.27	2.24	2.02	1.80
R410A	1.0	1.93	2.04	2.33	2.99	2.02	1.64	1.66
R410A/R22*	1.24	1.29	1.15	0.97	1.13	1.12	1.00	1.14

* Heat transfer coefficient ratio of R410A to R22

RESULTS AND DISCUSSION

Figs. 3-7 present the test results of evaporation of R22 and R410A in a smooth and seven microfin tubes. In Fig. 3, the evaporation heat transfer coefficients of R22 in the smooth tube are compared with the correlations [19-22]. The correlations of Shah [19] and Gungor and Winterton [20] underpredicted the measured data by 23%. Kandlikar's correlation [21] predicted well the test data within 7.7%, except the region with small refrigerant quality. Wattelet et al.'s correlation [22] is also predicted well the measured data within 8.7%, but the discrepancy increased with refrigerant mass flow rate.

Fig. 4 shows surface temperature profiles along the circumference for the microfin tube (MF-2) at the mass flow rate of 45 kg/h. The average surface temperatures of the tube were measured on the outer surface of the tube at three locations along the length of the tube mounted at the top, bottom, right and left of the tube in the circumferential direction. The temperatures of the top wall are higher than those of the bottom and side walls since the liquid film layer is thinner due to gravity. The circumferential variation of the wall temperatures for R22 is higher than that for R410A. The surface temperature of the top for R22 in small quality region ($x<0.4$) increases with quality. This is partly attributed to the specific volumes of R22 and R410A at the saturation temperature of 15°C. The specific volumes of saturated vapor and liquid for R22 at 15°C are 30% larger and 11% smaller than those for R410A, respectively, and therefore void fraction of R22 is higher than that for R410A at the same mass flow rate of 45 kg/h. As expected, surface temperature variations along the circumferential direction decrease as quality increases since the gravity and microfin effects become less important as flow pattern changes to annular flow.

Figs. 5 and 6 present local heat transfer coefficients of R22 and R410A at the mass flow rate of 45 kg/h, respectively. The incremental rate of heat transfer coefficients for MF-2, MF-3, MF-4 and MF-5 with quality is higher than that for other geometries (ST, MF-1, MF-6 and MF-7). The effect of quality on the heat transfer coefficients for the smooth tube is relatively small compared microfin tubes, suggesting the contribution of convective term to the heat transfer coefficient is small.

Fig. 7 shows average heat transfer coefficients for R22 and R410A, and Table 4 presents the heat transfer enhancement factor and the ratio of heat transfer coefficients of R410A to R22. Chamra et al. [8] defined the efficiency index (η)of the heat transfer coefficient for microfin tubes as

$$\eta = \frac{h / h_p}{\Delta P / \Delta P_p} \tag{8}$$

where subscript p indicates the plain tube. Since the pressure drop data are not available in this study, we defined the heat transfer enhancement factor as

$$\eta_h = h / h_p \tag{9}$$

The average heat transfer coefficients of microfin tubes for R22 and R410A are over 3.27 (MF-4) and 2.99 (MF-4) times higher than those for the smooth tube. The heat transfer coefficients for the cross-grooved tubes (MF-6, MF-7) are smaller than those for the single-grooved tubes except MF-1. This is opposite to Chamra et al.'s result [8] which the overall performance of the cross-grooved tube is greater than that of the single-grooved tube. It is attributed to the microfin geometries. The heat transfer coefficient increases with the fin height to inner diameter ratio (H_f/D_i)and the area ratio (A/A_p) and decreases with the helix and apex angles [1,2]. Note that H_f/D_i and A/A_p for MF-4 are the greatest along the single-grooved tubes and the apex and helix angles are the smallest as shown in Table 1.The heat transfer coefficients for R410A are larger than those for R22 except MF-3. This higher heat transfer performance attributed to the superiority of thermodynamic properties and nucleate boiling characteristics of R410A. The thermal conductivity of saturated vapor and liquid for R410A at 15°C are 13 and 19 % larger than those for R22, respectively.

CONCLUSION

An experimental study of R22 and R410A evaporation in the smooth and microfin tubes has been performed and the following conclusions are obtained.

(1) The measured heat transfer coefficients in the smooth tube are quite in agreement with Kandlikar's correlation within the rms error of ±7.7%.
(2) The circumferential variation of evaporation heat transfer coefficients for R22 is higher than that for R410A.
(3) The average evaporation heat transfer coefficients of R22 and R410A for the microfin tubes were 86-227% and 64-199%, respectively, higher than those for the smooth tube.
(4) When compared to R22 at the same test conditions, the evaporating heat transfer coefficients for R410A were 97-129% of R22.
(5) The incremental rate of heat transfer coefficient for the microfin tubes with refrigerant quality is greater than that for the smooth tube.

REFERENCES

1. Fujie, K., Itoh, M., Innami, T., Kimura, H., Nakayama, W. and Yanagida, T., "Heat transfer Pipe," *United States Patent*, Patent Number 4,044,797, 1977.
2. Shinohara, Y., Oizumi, K., Itoh, Y. and Hori, M., "Heat-Transfer Tubes with Grooved Inner Surfaces," *United States Patent*, Patent Number 4,658,892, 1987.
3. Yasuda, K., Ohizumi, K., Hori, M., and Kawamata, O., "Development of Condensing Thermofin-HEX-C Tube," *Hitachi Cable Review*, No. 9, pp. 247-252, 1990.
4. Schlager, L.M., Pate, M.B. and Bergles, A.E., "Evaporation and Condensation Heat Transfer and Pressure Drop in Horizontal, 12.7-mm Microfin Tubes with Refrigerant 22," *J. of Heat Transfer*, Vol.112, pp.1041-1047, 1990.
5. Kandlikar, S.G., "A Mmodel for Correlating Flow Boiling Heat Transfer in Augmented Tubes and Compact Evaporators," *J. of Heat Transfer*, Vol. 113, pp. 966-972, 1991.
6. Christoffersen, B.R., Chato, J.C., Wattelet, J.P, and Souza, A.L., "Heat Transfer and Flow Characteristics of R22, R32/R125 and R134a in Smooth and Microfin Tubes," *ACRC Technical Report* 47, University of Illinois at Urbana-Champaign, 1993.
7. Kaul, M.P., Kedzierski, M.A., and Didion, D.A., "Horizontal Flow Boiling of Alternative Refrigerants within a

Fluid Heated Microfin Tube," Process, Enhanced and Multiphase Heat Transfer: *A Fesischrift for A.E. Bergles*, Begell House, Inc., New York, pp.167-173, 1996.

8. Chamra, L., Webb, R, and Randlett, M., "Advanced Microfin Tubes for Evaporation," *Int. J. Heat Mass Transfer*, Vol. 39, No. 9, pp. 1827-1996, 1996.
9. Kuo, S.C. and Wang, C.C., "In-tube Evaporation of HCFC-22 in a 9.52 mm Microfin/Smooth Tube," *Int. J. Heat Mass Transfer*, Vol. 39, No. 12, pp. 2559-2569, 1996.
10. Liu, X, "Condensing and Evaporating Heat Transfer and Pressure Drop Characteristics of HFC-134a and HCFC-22," *J. of Heat Transfer*, Vol. 119, pp.158-163, 1997.
11. Uchida, M., Itoh, M., Shikazono, N., and Kudoh, M., "Experimental Study on the Heat Transfer Performance of a Zeotropic Refrigerant Mixture in Horizontal Tubes," *Proc. of 1996 Int. Refrigerant Conference at Purdue*, pp. 133-138, 1996.
12. Yamamoto, Y., Miyamura, Y., Nasako, K., Matsumoto, K., and Osumi, M., "Evaporation Heat Transfer Characteristics of Refrigerant Mixtures in Horizontal Tubes," *Proc. of the 34th Japanese Heat Transfer Symposium*, pp. 485-486, 1997.
13. Kattan, N., Thome, J.R. and Favrat, D., "Flow Boiling in Horizontal Tubes: Part III – Development of a New Heat Transfer Model Based on Flow Pattern," *J. of Heat Transfer*, Vol. 120, pp. 156-165, 1998.
14. Boissieux, X., Heikal, M.R. and Johns, R.A., "Two-phase Heat Transfer Coefficients of Three HFC Refrigerants Inside a Horizontal Smooth Tube, Part I: Evaporation, " *Int. J. of Refrigeration*, Vol. 23, pp. 269-283, 2000.
15. Wilson, E.E., "A Basis for Rational Design of Heat Transfer Apparatus," *ASME Trans*., Vol.37, pp.47-82, 1915.
16. Briggs, D.E. and Young, E.H., "Modified Wilson Plot Techniques for Obtaining Heat Transfer Correlations for Shell and Tube Heat Exchangers," *Chem. Eng. Prog. Symp. Ser.*, Vol.65, No.92, pp.35-45, 1969.
17. Huber, M., Gallagher, J., McLinden, M., and Morrison, G., NIST Thermodynamic Properties of Refrigerants and Refrigerant Mixtures Database (REFPROP), Version 5.1, NIST, 1996.
18. Moffat, R.J., "Describing the Uncertainties in Experimental Results," *Exp. Thermal and Fluid Science*, Vol. 1, pp. 3-17, 1988.
19. Shah, M.M., "Chart Characteristics for Saturated Boiling Heat Transfer: Equation and Further Study," *ASHRAE Trans.*, Vol.88, Pt.1, pp.185-196, 1982.
20. Gungor, K.E. and Winterton, R.H.S., "A General Correlation for Flow Boiling in Tubes and Annuli," *Int. J. Heat Mass Transfer*, Vol.29, pp.351-358, 1986.
21. Kandlikar, S.G., "A General Correlation for Saturated Two-phase Flow Boiling Heat Transfer Inside Horizontal and Vertical Tubes," *J. of Heat Transfer*, Vol.112, pp.219-228, 1990.
22. Wattelet, J.P, Chato, J.C., Souza, A.L., and Christofferson, B.R., "Evaporative Characteristics of R12, R134a, and a Mixture at Low Mass Fluxes," *ASHRAE Trans*., Vol.100, Pt.1, pp.603-615, 1994.